Two-dimensional photon counting imaging detector based on a Vernier position sensitive anode readout *

YAN Qiu-Rong(鄢秋荣)[1,2;1)] ZHAO Bao-Sheng(赵宝升)[1] LIU Yong-An(刘永安)[1]
YANG Hao(杨颢)[1,2] SHENG Li-Zhi(盛立志)[1] WEI Yong-Lin(韦永林)[1]

[1] State Key Laboratory of Transient Optics and Photonics, Xi'an Institute of Optics and Precision Mechanics, Chinese Academy of Sciences, Xi'an 710119, China
[2] Graduate University of Chinese Academy of Sciences, Beijing 100049, China

Abstract: A two-dimensional photon counting imaging detector based on a Vernier position sensitive anode is reported. The decode principle and design of a two-dimensional Vernier anode are introduced in detail. A photon counting imaging system was built based on a Vernier anode. The image of very weak optical radiation can be reconstructed by image processing in a period of integration time. The resolution is superior to 100 μm according to the resolution test. The detector may realize the imaging of very weak particle flow of high-energy photons, electrons and ions, so it can be used for high-energy physics, deep space exploration, spectral measurement and bio-luminescence detection.

Key words: photon counting imaging, Vernier anode, micro-channel plate, particle detection

PACS: 29.40.Cs, 29.40.Gx **DOI:** 10.1088/1674-1137/35/4/009

1 Introduction

Photon counting imaging is a kind of imaging detection method for very weak light. The micro-channel plate (MCP) detector with a position sensitive anode readout can provide a photon counting imaging capability. Although the intensifier coupled CCD (ICCD) and electron multiplying CCD (EM-CCD) can also work in photon counting mode, they require that the CCD has a very high frame rate and very low circuit noise, so deep cooling is a necessity and the manufacturing cost is not modest [1]. The MCP detector with a position sensitive anode readout has many advantages, such as a high signal to noise ratio, high sensitivity, a wide dynamic range and good resistance to drift.

The MCP photon counting imaging detector consists of two parts: the MCP stack and the position sensitive anode readout. The MCP stack converts the incident photon into a charge cloud. The anode readout decodes the centroid of the charge cloud, which corresponds to the coordinates of the incident photon. The MCP can directly respond to part of the high-energy photons, electrons and ions. For example, in the soft X-ray and UV band of 30–110 nm, the MCP has a quantum efficiency of 5%–15%. The application can also be extended to other bands by depositing a photocathode on the input surface of the MCP. Photon counting imaging based on the MCP can realize the imaging of a very weak particle flow of high-energy photons, electrons and ions, so it can be used for high-energy physics, deep space exploration, spectral measurement and bio-luminescence detection [2–3]. MCPs have been relatively well developed, while the study of high-performance anodes still needs more work. There are several types of position sensitive anode [4] that have been investigated, such as WSA [5], delay line [6], cross strip [7] and multi-anode microchannel array (MAMA) [8]. Compared with the above mentioned anodes, the Vernier anode shows very high spatial resolution and imaging linearity.

In this paper, a two-dimensional photon counting imaging detector based on a Vernier position sensitive anode is reported. The decoding principle and design of a two-dimensional Vernier anode are introduced in

Received 23 June 2010, Revised 1 September 2010
* Supported by Key Program of National Natural Science Foundation of China (10878005)
1) E-mail: yanqiurong@opt.ac.cn

detail. A photon counting imaging system was built, based on a detector with a Vernier anode read out. The resolution of the detector was tested and the experimental results were analyzed in detail.

2 Decoding principle and design of a Vernier anode

The original Vernier anode pattern was described by Lapington [9]. Several different Vernier anode structures have been developed, such as a one-dimensional Vernier with six electrodes, a two-dimensional Vernier with twelve electrodes and a two-dimensional Vernier with nine electrodes. It is theoretically demonstrated that a two-dimensional Vernier anode with nine electrodes can achieve a position resolution of 10 μm and the imaging performance is limited by the MCP pore spacing [10]. The Vernier anode and supporting electronics are responsible for determining the centroid of the charge cloud and thus the imaging resolution. Depending on the exact performance of the electronic read out, these Vernier [9–11] anodes achieve imaging resolutions of between 25 μm and 100 μm.

As shown in Fig. 1, the basic electrode unit of a Vernier anode is a rectangular strip, which is divided into three strips by two sine insulated channels, G_1 and G_2. The two sine channels have the same period, the same amplitude and a fixed phase shift. Along the X axis, the width of three strips, A_1, A_2, A_3 change periodically, and can be described as follows,

$$A_1 = \frac{N}{3} + \frac{N}{3}\sin(\theta_A + \varphi), \tag{1}$$

$$A_2 = \frac{N}{3} + \frac{N}{3}\sin\left(\theta_A - \frac{2\pi}{3} + \varphi\right), \tag{2}$$

$$A_3 = \frac{N}{3} + \frac{N}{3}\sin\left(\theta_A - \frac{4\pi}{3} + \varphi\right), \tag{3}$$

where N is the width of rectangular strip and φ is the initial phase of sine insulated channel G_1. $\theta_A = \dfrac{2\pi}{\lambda_A}x$, λ_A is the wavelength of the sine insulated channel, so θ_A corresponds to the x coordinates.

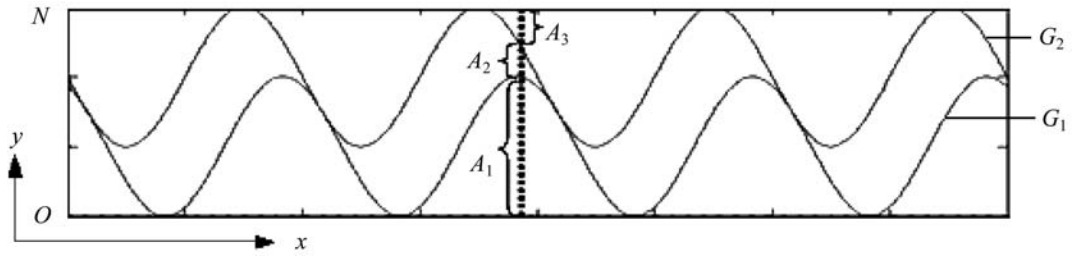

Fig. 1. The basic electrode unit of a Vernier anode.

Figure 2 shows the electrode structure of a two-dimensional Vernier anode with nine electrodes. Three basic electrode units, A, B and C, with different wavelengths of a sine insulated channel, are arranged in an interlaced way, and they constitute the two-dimensional electrode pattern. One set of A, B and C electrode units is called a pitch. Fig. 2 shows only three pitches. Strips $A1$, $A2$ and $A3$ form the electrode unit A, Strip $B1$, $B2$ and $B3$ form unit B, and Strip $C1$, $C2$ and $C3$ form the electrode unit C. Strips of the same name are connected together as one output, so two-dimensional Vernier anodes have nine outputs $A1$, $A2$, $A3$, $B1$, $B2$, $B3$, $C1$, $C2$ and $C3$. The phases of the same electrode unit shift linearly along the y axis. The line in Fig. 2 is the phase line of the electrode unit group A. When the charge cloud is collected by electrode unit A, the area of its three anode strips covered by the charge cloud can be expressed, respectively, by the following expressions.

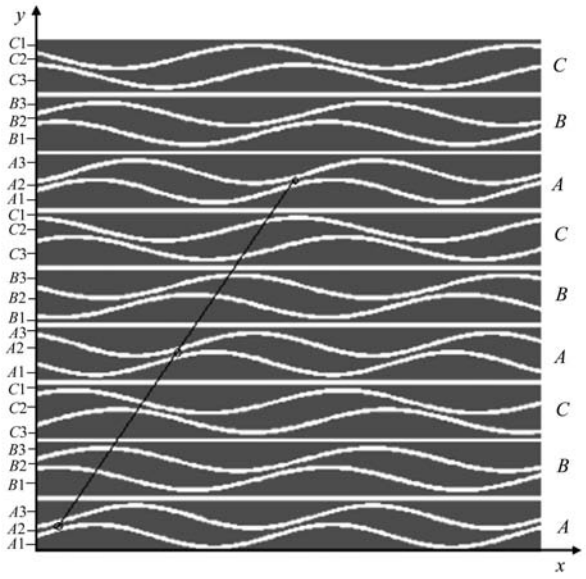

Fig. 2. The electrode structure of a two-dimensional Vernier anode with nine electrodes.

$$S_{A1} = \int_{\theta_0-\frac{\Delta\theta}{2}}^{\theta_0+\frac{\Delta\theta}{2}} \left[\frac{N}{3}+\frac{N}{3}\sin(\theta_A+\varphi)\right]\mathrm{d}\theta, \quad (4)$$

$$S_{A2} = \int_{\theta_0-\frac{\Delta\theta}{2}}^{\theta_0+\frac{\Delta\theta}{2}} \left[\frac{N}{3}+\frac{N}{3}\sin\left(\theta_A-\frac{2\pi}{3}+\varphi\right)\right]\mathrm{d}\theta, \quad (5)$$

$$S_{A3} = \int_{\theta_0-\frac{\Delta\theta}{2}}^{\theta_0+\frac{\Delta\theta}{2}} \left[\frac{N}{3}+\frac{N}{3}\sin\left(\theta_A-\frac{4\pi}{3}+\varphi\right)\right]\mathrm{d}\theta, \quad (6)$$

where θ_0 is the corresponding phase of centroid of the charge cloud, and $\Delta\theta$ is the phase width corresponding to the diameter of the charge cloud. Because the charge collected by the anode is proportional to the area of the anode covered by the charge cloud, θ_0 will give information about the charge cloud centroid and then the neutron interaction position. If N is small enough, the number of electrode units A arranged in the plane area is large. It can be considered that any point (x, y) at the two-dimensional plane corresponds to one phase θ_A. Similarly, any point (x, y) at the two-dimensional plane corresponds to phase θ_B and θ_C. Fig. 3 shows the phase distribution of θ_A, θ_B and θ_C in a two-dimensional plane, respectively, therefore the three phases of θ_A, θ_B and θ_C can be used to calculate the two-dimensional coordinates.

Through theoretical analysis and calculation, we define $\theta_A+\theta_B = \theta_x$, $\theta_B+\theta_C=\theta_y$. Provided that the wavelength and the initial phase of the sine-channels meet certain relations, θ_x and θ_y will change periodically along the x-axis and y-axis, respectively. The distribution of θ_x, θ_y in a two-dimensional plane is shown in Fig. 4, therefore, based on two phases, θ_A and θ_B, θ_x can be calculated. θ_x has periodicity corresponding to the x coordinate. Fig. 4(a) shows that one θ_x corresponds to three x coordinates. Similarly, θ_y has periodicity and one θ_y corresponds to three y coordinates, as shown in Fig. 4(b).

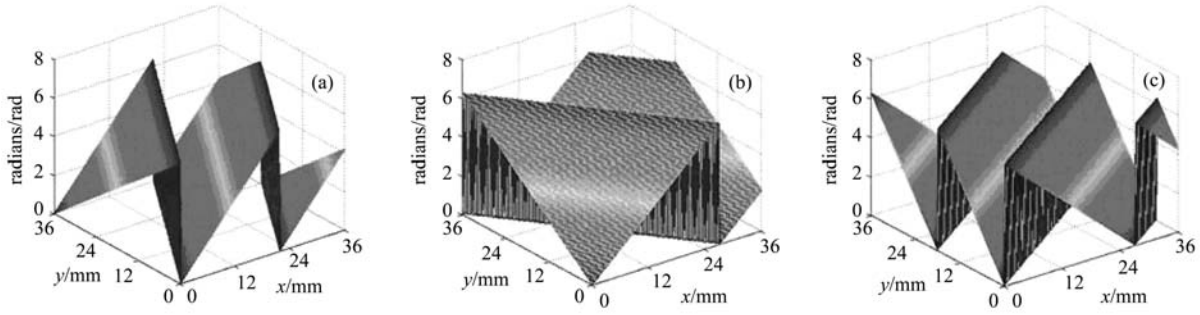

Fig. 3. (a) The phase distribution of θ_A in a two-dimensional plane; (b) the phase distribution of θ_B in a two-dimensional plane; (c) the phase distribution of θ_C in a two-dimensional plane.

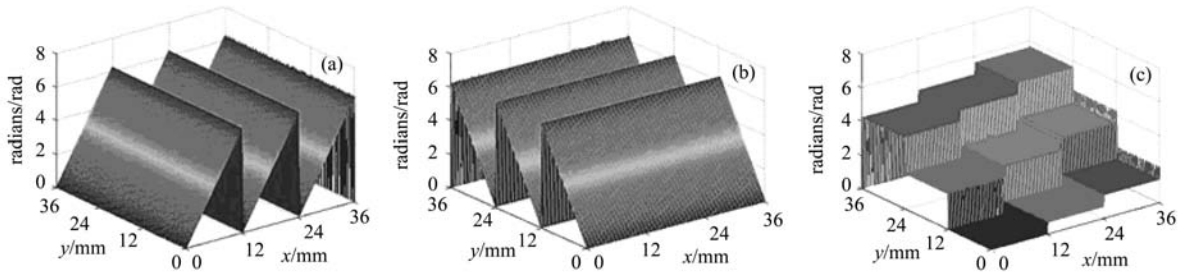

Fig. 4. (a) The phase distribution of θ_x in a two-dimensional plane; (b) the phase distribution of θ_y in a two-dimensional plane; (c) the phase distribution of θ_z in a two-dimensional plane.

According to θ_x and θ_y, the precise position in one period can be calculated. This is the first step of decoding. The second step is to determine the coordinates in which period by constructing the equation as follows,

$$\theta_z = \theta_A+\theta_C-\theta_x/n^2-\theta_y/n, \quad (7)$$

where n is the number of period. When n=3, the distribution of θ_z in a two-dimensional plane is shown in Fig. 4(c). The plane is divided into nine regions, and each region represents a discrete value. These discrete values of θ_z can be expressed by the matrix, as follows,

$$\begin{bmatrix} 0 & \frac{2\pi}{n} & \cdots & \frac{2(n-1)\pi}{n} \\ \frac{2\pi}{n^2} & \frac{2(n+1)\pi}{n^2} & \cdots & \\ & & \cdots & \\ \frac{2(n-1)\pi}{n^2} & \frac{2(n-1)\pi}{n^2} & & \frac{2(n^2-1)\pi}{n^2} \end{bmatrix}.$$

Decoding of a Vernier anode can be expressed by the following two formulas,

$$x = \lambda_x \frac{\theta_x}{2\pi} + i\lambda_x, \tag{8}$$

$$y = \lambda_y \frac{\theta_y}{2\pi} + j\lambda_y, \tag{9}$$

where λ_x is the periodic length along the x axis, λ_y is the periodic length along the y axis, and i and j are the index value of elements of the matrix. The decoding of a Vernier anode consists of two steps. The first step, called "fine tuning", is used to calculate two-dimensional coordinates in a periodic region. The second step called "coarse tuning" is used to calculate the index value according to the value of θ_z.

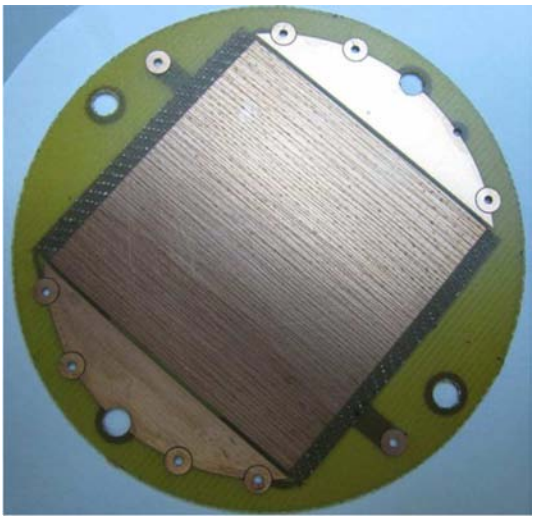

Fig. 5. Photograph of a Vernier anode.

Figure 5 shows a Vernier anode developed by us. It was produced by micro-electronics technology. The insulating substrate is a PCB board and the conductive layer is copper. Both the length and the width of the anode collection area are 36 mm. The thickness of the conductive layer is 5 μm, the width of the insulated channels is 20 μm and the minimum width of the anode is 30 μm.

3 Experimental setup

Figure 6 shows the photon counting imaging experimental system based on a two-dimensional Vernier anode. The experimental system is composed of a single-photon source, a Vernier detector, an electronic read-out systems, data acquisition cards and a computer. The single-photon source consists of a mercury lamp, several attenuators and a narrow-band optical filter. The single-photon source radiates very weak 253.7 nm UV photons. The mask on the input surface of the MCP is used to simulate the image of the focal plane. Photoelectric conversion occurs in the input surface of the MCP, and a photoelectron is emitted by a certain quantum efficiency. After passing through the MCP arranged in a V-shaped cascade, the photoelectron is multiplied and forms a charge cloud with multiplication factors of 10^6–10^7. After being accelerated by the electric field between the MCP and the anode, the charge cloud is collected by the Vernier anode. The nine electrode outputs of the Vernier anode export charge signal. The charge signal is converted into a voltage signal by a charge sensitive preamplifier [12], and the output signal of the preamplifier is fed into the shaping amplifier, where the pulse is shaped as a quasi-Gaussian to optimize the S/N ratio of the system. The quasi-Gaussian pulse enters the PCI data acquisition card,

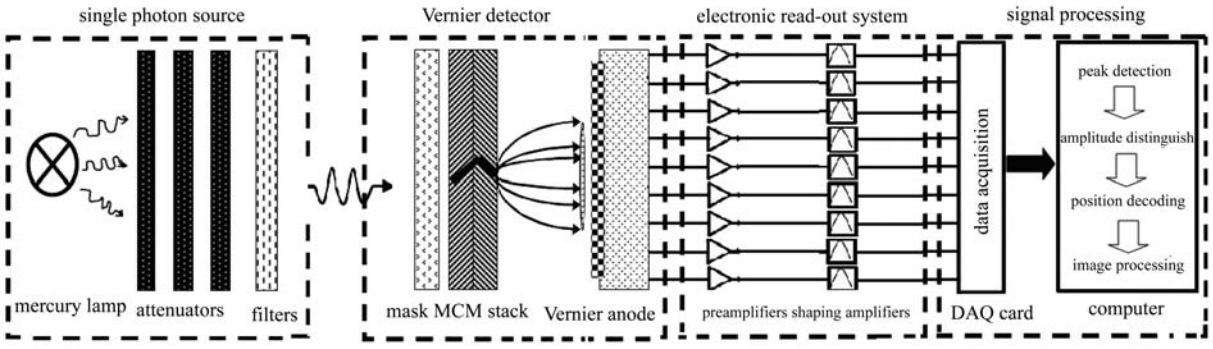

Fig. 6. The photon counting imaging experimental system based on a two-dimensional Vernier anode.

where continuous and high-speed data acquisition is performed at the sample rate of 5 MHz. Computer software finds the pulse's peak voltage, which reveals the information of the two-dimensional coordinates of each single photon event with a series of signal processing methods, such as noise filtering, peak detection, amplitude distinguishing and pulse pileup rejection. The two-dimensional coordinates of single photon events are calculated. According to the counts of single-photon events at different locations, a gray image can be generated by image processing technology.

4 Experimental results and analysis

4.1 Operating voltage of the MCP

The operating voltage of the MCP affects the resolution of the detector. Fig. 7 shows the pulse height distribution when the MCP works at different voltages. When the MCP works at non-saturation of 1600 V, the pulse height distribution is a negative exponential distribution. This shows that most single-photon pulses have a smaller amplitude. When the MCP works in the saturated voltage of 2000 V, the pulse height distribution is a Gaussian distribution, indicating that the amplitude of a single-photon pulse is concentrated in a certain range. The output pulses of the detector also include a small number of noise pulses, besides the signal pulses on behalf of the single-photon events. Most of the noise pulses caused by dark current have a smaller amplitude, and the noise pulses caused by high-energy particles, such as cosmic rays, have a larger amplitude. The noise signal pulses can be partly rejected by setting the maximum threshold and minimum threshold, as much as possible to retain single-photon pulses and to gain a higher signal to noise ratio. Therefore, a higher resolution would be available when the MCP stack works in saturation. The experimental results show that the detector has the best resolution when the MCP stack works in a saturated voltage of 1900 V with a maximum threshold value of 11 V and a minimum threshold value of 2 V.

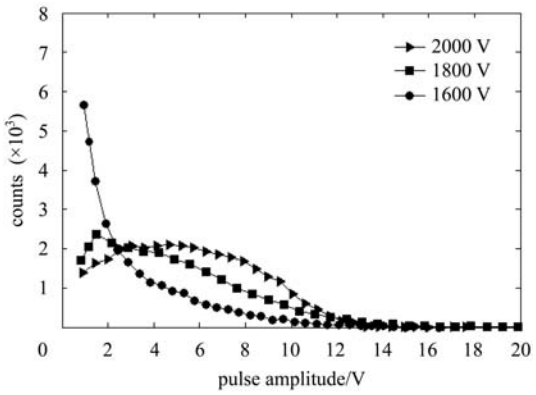

Fig. 7. Pulse height distribution curves when working at different voltages.

4.2 Size of charge cloud

The size of the charge cloud collected by the Vernier anode is the key factor affecting the resolution. If the charge cloud is too small, the number of pitches covered by the charge cloud is fewer, and then the resolution of the location of the centroid is worse. If the charge cloud is too large, it will be beyond the edge of the anode, so the charge collection is incomplete and the effective detection area will be affected finally. On the other hand, as the electrons of the charge cloud do not show uniform distribution, but show Gaussian distribution, the charge collected by the anode is not linearly proportional to the area of the anode when the charge cloud is too large. This will lead to inaccurate decoding of the coordinates. The diameter of the charge cloud can be expressed by [13]

$$D = kd\sqrt{\frac{E_{\rm e}}{V_{\rm a}}}, \tag{10}$$

where D(mm) is the diameter of the charge cloud, k is the proportional coefficient, d(mm) is the distance from the MCP to the anode, $V_{\rm a}$ (V) is the acceleration voltage between the MCP and the anode, and $E_{\rm e}$ (eV) is the initial energy of the electron. The distance from the MCP to the anode is the key factor affecting the size of the charge cloud, so a better resolution can be obtained by adjusting the distance between the MCP and the anode. Experimental results show that the resolution of the detector is best when the distance between the MCP and the anode is 18 mm. According to the methods of estimating the charge cloud size proposed by Zhang [14], the diameter of the charge cloud is estimated to be about 11 mm.

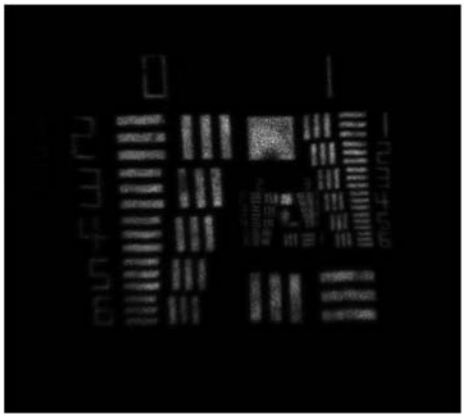

Fig. 8. Image of the USAF 1951 mask taken by the experimental system.

4.3 Resolution test

To test the spatial resolution of the detector, we set the USAF 1951 resolution mask close to the input surface of the MCP to simulate the image of the focal plane. When the distance between the MCP and the anode is 18 mm, the MCP stack works in a saturated voltage of 1900 V, the Maximum threshold value is set to 11V, the minimum threshold value is set to 2 V and the data acquisition time is 30 minutes. An image of the mask taken by the experimental system is shown in Fig. 8. The center of the image has very good linearity. The uneven distribution of image brightness is due to the uneven nature of the incident light. The imaging result shows that the resolution is better than 100 μm.

5 Conclusion

A photon counting imaging detector based on a two-dimensional Vernier anode is developed. A single photon imaging system based on a Vernier anode is established. The image of the ultra-weak radiant source can be reconstructed in a period of time. The experimental results show that the decoding algorithm and the design of the Vernier anode are correct, and they reveal that a superior spatial resolution is 100 μm according to the resolution test results. The detector can realize the imaging of very weak particle flow of high-energy photons, electrons and ions, so it can be used for high-energy physics, deep space exploration, spectral measurement and bio-luminescence detection.

References

1 David D, Paul H. Proc. SPIE, 2004, **5563**: 159
2 SUN X L, Krainak M A, Abshire J B et al. J. Mod. Opt., 2004, **51**: 1333
3 Gallivanoni A, Rech I, Resnati D et al. Opt. Express, 2006, **14**: 5021
4 WANG Xiao-Hu, ZHU Qi-Ming, CHEN Yuan-Bo et al. Chinese Physics C (HEP & NP), 2008, **32**(11): 903
5 MIAO Zhen-Hua, ZHAO Bao-Sheng, ZHANG Xing-Hua et al. Chinese Physics Letters, 2008, **25**(7): 2698
6 Czasch A, Milnes J, Hay N et al. Nucl. Instrum. Methods A, 2007, **580**: 1066
7 Siegmund O H W, Tremsin A S, Vallerga J V et al. Nucl. Instrum. Methods A, 2003, **504**: 177
8 FENG Bing, KANG Ke-Jun, WANG Kui-Lu et al. Nucl. Instrum. Methods A, 2004, **535**: 546
9 Lapington J S, Sanderson B, Worth L B C et al. Nucl. Instrum. Methods A, 2002, **447**: 250
10 Lapington J S, Sanderson B. Proc. SPIE, 2000, **4139**: 242
11 Lapington J S. Proc. SPIE, 2003, **4854**: 191
12 FENG Lang, GE Yu-Cheng, WANG He et al. Chinese Physics C (HEP & NP), 2009, **33**(1): 50
13 Grantham S E, Miesak E, Reese P et al. Proc. SPIE, 1994, **2273**: 108
14 ZHANG Xing-Hua, ZHAO Bao-Sheng, ZHAO Fei-Fei et al. Rev. Sci. Instrum., 2009, **80**: 033101